URSI GASS 2021, Rome, Italy, 28 August - 4 September 2021

Accurate Geometrical Modeling and Field-to-Wire Coupling Prediction in Wiring-Structures with Loops

X. Liu[(1)], F. Grassi[(1)], G. Spadacini[(1)], and S. A. Pignari[(1)]
(1) Politecnico di Milano, Department of Electronics, Information and Bioengineering, Milan 20133, Italy

Abstract

Irregular-shaped wiring structures are usually encountered in practical applications. In this work, a wiring structure encompassing a loop is modeled geometrically by resorting to a 3D cylindrical helix. To predict the disturbances induced by an incident electromagnetic field at the terminals of such a nonuniform structure, a simplified numerical solution based on transmission-line (TL) theory is developed. To this end, the structure is discretized in segments and the Agrawal TL model is formulated by accounting for the actual orientation of each wire segment with respect to the incident electric field vector. Full-wave simulations of the current induced in the terminations of the wiring structure under analysis are used to validate the accuracy of the proposed numerical TL-based method as well as its computational effectiveness.

1 Introduction

Cable harnesses are widely encountered in industrial applications, and are often regarded as critical parts of the system due to their ability to pick-up electromagnetic (EM) noise. Hence, it is of paramount importance to accurately account for possible nonuniformity of cable geometry as well as for the possible complexity of the electromagnetic environment [1], while predicting the noise expected at the terminations of wiring structures. In the last decade, several research works have been done, e.g. [1]-[4], with the aim to model irregularly-shaped wire harnesses and to address pertinent Electromagnetic Compatibility (EMC) issues.

In this paper, a wiring structure with a loop in the middle, which is commonly encountered in practice, is modeled with the objective to predict its EMC performance. For geometrical modeling of the loop, the 3-D analytical expression of a cylindrical helix [5] is exploited, followed by proper rotation and translation. Straight wires are subsequently tied to both ends for terminal connection.

For radiated susceptibility study, full-wave 3D solvers are the most accurate to account for the irregular wiring geometry and to predict the induced noise at terminal ends caused by an arbitrary incident field. Conversely, non-uniform transmission line (NUTL) methods resorting to transmission line (TL) theory provide just approximated predictions, however, their unparalleled computationally efficiency makes them the preferred solution for industrial needs [6]. Though the TL models developed in previous works, e.g. [1], [2], are effective for cable harnesses running (at least approximately) parallel to a metallic ground plane, their applicability to wiring structures involving loops is critical, due to the simplifications made to derive the distributed sources introduced by the impinging EM field, which do not account for the mutual orientation of the wire and the electric field.

To overcome this limitation, in this work the analytical Agrawal model in [7] is reformulated by accounting for the local wire orientations in 3-dimensions to evaluate the distributed excitation sources induced by the external field. By varying the parameters defined for controlling the loop geometry, different scenarios are investigated, and several insights into the noise expected at the terminations of the structure under analysis are provided. On the whole, the obtained results demonstrate the effectiveness and feasibility of the proposed geometry modeling procedure and the TL-based field-to-wire coupling model. Also, they confirm the need to accurately model the geometry of the wiring structure in order to obtain reliable estimates of the actual interference levels. For instance, it will be proven that neglecting the presence of loops may lead to underestimation of the actual interference level especially at high frequency.

2 Modeling of the Wiring Structure

The nonuniform wiring structure under investigation (see Fig. 1) encompasses a loop in the middle with straight wires connected by the side. To avoid self-intersection of the geometry and better reproduce the physical shape, the loop is modeled as a single turn of a helix instead of an arc.

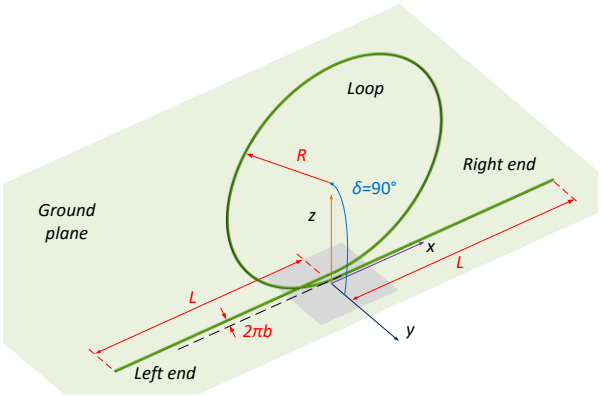

(a)

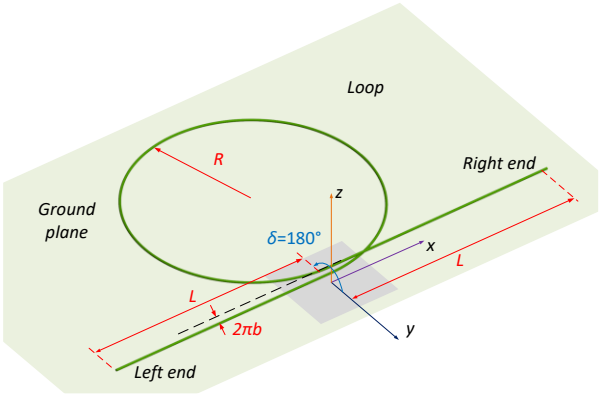

(b)

Figure 1. Illustration of the studied wire-loop structure, outlining the parameters introduced to control the loop geometry. (a) δ=90°, and (b) δ=180°.

For a general cylindrical helix parameterization in Cartesian coordinates [5], two parameters, R and b, are introduced to control the radius and the pitch of the loop, respectively. This leads to:

$$\begin{cases} x'(t) = bt \\ y'(t) = R\sin(t) \\ z'(t) = R\cos(t) \end{cases} \tag{1}$$

with $-3\pi/2 \le t \le \pi/2$ for a single loop. With reference to Fig. 1, by introducing δ to describe the loop rotation with respect to ground (i.e., $0° \le \delta \le 180°$ when the loop is parallel to the ground or rotated upward w.r.t. the terminal ends) and h_0 to describe the structural height above ground, the loop coordinates write:

$$\begin{bmatrix} x(t) \\ y(t) \\ z(t) \end{bmatrix} = \begin{bmatrix} \sin\left(\delta + \pi/2\right) & \cos\left(\delta + \pi/2\right) & 0 \\ \cos\left(\delta + \pi/2\right) & -\sin\left(\delta + \pi/2\right) & 0 \\ 0 & 0 & 1 \end{bmatrix} \begin{bmatrix} x'(t) \\ y'(t) \\ z'(t) \end{bmatrix} + \begin{bmatrix} h_0 \\ 0 \\ 0 \end{bmatrix} \tag{2}$$

After obtaining the loop structure, straight wire sections with length L are subsequently connected at both ends of the loop. For full-wave simulation in a commercial EM solver, additional vertical wire segments are further connected at the terminations of the straight-wire sections where terminal impedances are included.

3 Radiated Susceptibility Prediction Model

For field-to-wire coupling prediction, the generated parametric representation of the geometry can be then imported into a full-wave electromagnetic solver to obtain predictions of the induced noise at the terminal ends. Though accurate, full-wave simulations require non-negligible computation burden, especially for complex geometries. As an alternative solution, the structure is here discretely sampled and solved by resorting to TL theory in combination with the uniform cascade section (UCS) method [6], with a special concern on the evaluation of distributed sources introduced by the external field.

As a matter of fact, the numerical models available in the literature, e.g. [1], were developed by assuming the axis of the wiring structure nearly parallel to ground. Accordingly, the evaluation of the distributed sources representative for field-to-wire coupling [7] is usually simplified by (a) approximating the arbitrary incident field as linear interpolations based on sampled positions, and (b) considering the directions of wire segment limited to the longitudinal axis only. Although effective as long as wire harnesses are nearly parallel to ground, the involved simplifications cannot be adopted for structures exhibiting high non-uniformity with respect to ground, as it will be shown in the next Section.

Focusing on this issue, the solution approach adopted in this work makes use of a refined discretized geometry. Consequently, the field horizontal- and vertical-components are also considered for accurate projection onto wire trajectories. Besides, for characterizing transmission properties the actual length of wire segments instead of their longitudinal length is considered, as these quantities can be significantly different due to line non-uniformity w.r.t. ground.

To this end, the procedure to evaluate the distributed sources due to the longitudinal contribution of the EM field in [1] is here reformulated as follows:

1) The coefficients a, b, c, and d used for piecewise-linear interpolation of the longitudinal (z-axis) field component, corresponding to (16)-(19) in [1], are analogously obtained for the horizontal (y-axis) and vertical (x-axis) components;

2) Additionally, for each wire segment in the previous step, a weight parameter is calculated per direction as the ratio of the projection length in that direction to the actual length;

3) The coefficients and weights calculated in previous steps are considered together in the subsequent calculation of the longitudinal contribution, i.e., (21)-(22) in [1];

4) Longitudinal lengths are replaced by actual wire lengths in (23)-(25) of [1].

4 Simulation and Discussion

In this Section, the proposed modeling scheme is validated by simulation. To this end, a radiated-susceptibility test setup, where the wiring structure under analysis is

illuminated by an incident plane-wave field (see Fig. 2) characterized by E-field strength E_0=1 V/m and incidence angles ϑ=50°, η=60°, ψ=20° are considered. The conductor radius is 0.25 mm, and the insulation coating is not considered here for simplicity. The height, h_0, is properly chosen for each test case, such that the right-end terminal wire runs at a constant height of 5 mm above the perfect metallic ground. The left-end terminal wire has a fixed y-coordinate of 0. It is worth noticing that the choice of a lower height above ground further increases line nonuniformity, thus strengthening the value of the proposed validation. Both wire terminals are connected to ground through an impedance Z=220 Ω.

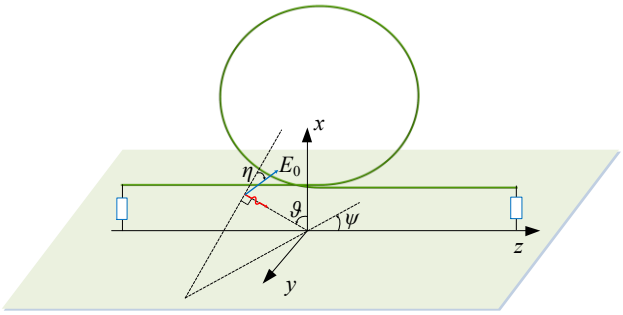

Figure 2. Principle drawing of the wiring structure under analysis, illuminated by an external plane-wave field.

First, a reference structure is generated, which is characterized by the parameters R=5 cm, b=0.5 mm, and δ=180°. Besides, short terminal ends with L=1 cm are chosen to increase line non-uniformity with respect to ground. For this structure, predictions of the current induced at the left terminal (see Fig. 3) show a satisfactory agreement up to 2 GHz between the proposed TL-based model and full-wave simulation (by the Method of Moments, MoM) despite the strong non-uniformity affecting the wiring structure. Conversely, if the evaluation of the field is made by adopting the same simplifications which are feasible and usually adopted by the models in the literature for wiring structures nearly parallel to ground, the result (see the red curve in Fig. 3) exhibits less accuracy in the whole frequency range, due to inaccurate modeling of the distributed sources.

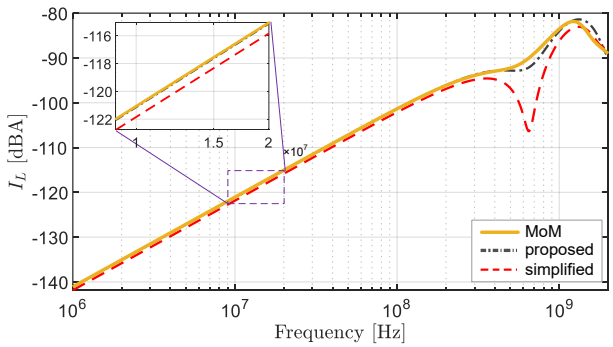

Figure 3. Prediction of the current induced at the left terminal (reference structure with: R=5 cm, b=0.5 mm, δ=180°, and L=1 cm).

Besides, the proposed method is proved to notably reduce the calculation time w.r.t the full-wave simulation. As a matter of fact, for simulation on a standard desktop PC with an Intel(R) Core(TM) i5-7400 CPU running at 3.0 GHz and 16 GB of RAM, the MoM simulation with fine meshing scheme takes 347.0 s, while the proposed method using a uniform sampling of 1,000 sections per meter takes only 5.5 s, with an additional time of 3.2 s for numerical evaluation of pertinent per-unit-length parameters. In both cases, a discrete-frequency sampling (i.e., 100 points/decade, that is 431 points to cover the frequency range from 100 kHz up to 2 GHz) is adopted.

For different loop radii R, predictions of the current induced at the left terminal are compared in Fig. 4. In these simulations, the wire length was chosen equal to L=0.1 m to represent a more practical realization, and b is chosen to be 0.5 mm. When δ=180° [see Fig. 4(a)], that is the loop is oriented parallel to the ground, the amplitude of the current induced at the left end gradually increases with R at low frequencies. Also, the high-frequency resonances shift toward lower frequencies, due to the increase of the actual wire length. Besides, it can be observed that neglecting the presence of the loop [situation denoted as R=0 cm in Fig. 4(a)] can lead to non-negligible underestimations of the current induced at terminals, especially at high frequency. When the loop is orthogonal to the ground, that is for δ=90° [see Fig. 4(b)], interpretation of the obtained results is not so straightforward. Indeed, though not shown here, with the increase of R, the left-end current, which was initially larger for R=1 cm, becomes smaller than the right-end current for R=3 cm and R=5 cm. In spite of that, the proposed method is proven to be able to provide predictions in good agreement with full-wave simulation in the whole frequency interval of interest.

Eventually, Fig. 5 compares the predictions of the induced current for different loop pitches. For these simulations the values R=3 cm and L=0.1 m were adopted. The obtained results confirm the effectiveness of the proposed solution technique. For both loop orientations (i.e., δ=180° and δ=90°), the induced current increases with b, as it is especially evident for δ=180°. For larger pitches, the loop area increases accordingly, and this contributes to increase of the noise induced at the line terminals. In passing, it is worth mentioning that low-frequency prediction is more accurate with a larger pitch. This feature is readily appreciable by observing the zoomed range shown in Fig. 5(b). Indeed, spurious cross-coupling (i.e., crosstalk) among adjacent parts of the structure (effect which is expected to be more evident at the loop ends and which cannot be accounted for by the proposed model) plays a weaker role if the loop pitch increases, since the separation between the loop ends increases. As a result, the discrepancies between TL-based predictions and full-wave simulations decrease.

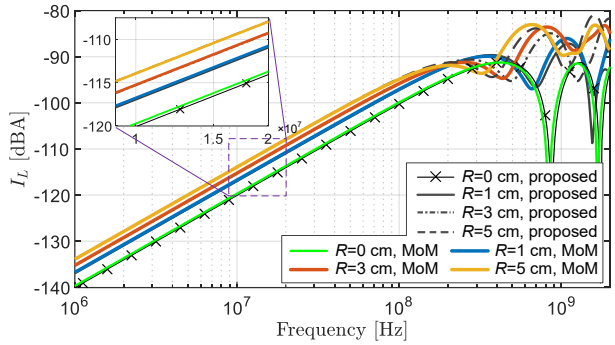

(a)

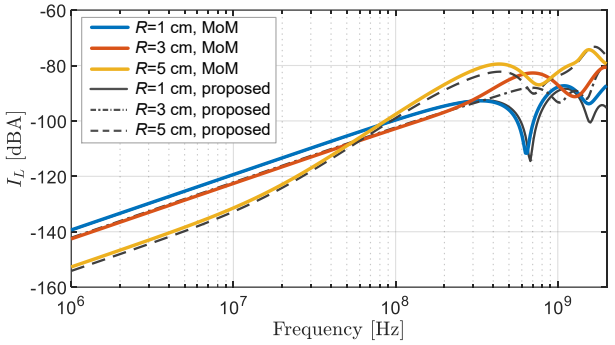

(b)

Figure 4. Prediction of the current induced at the left terminal for different loop radii R (b=0.5 mm and L=0.1 m) for (a) δ=180°, and (b) δ=90°.

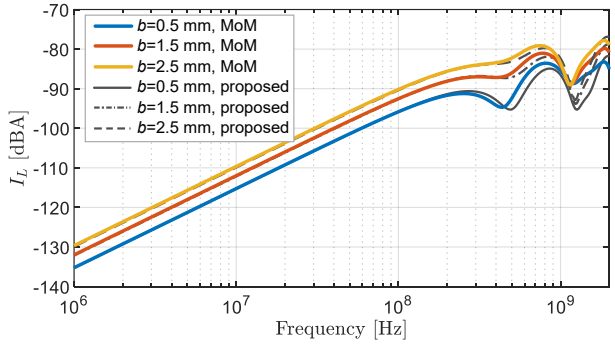

(a)

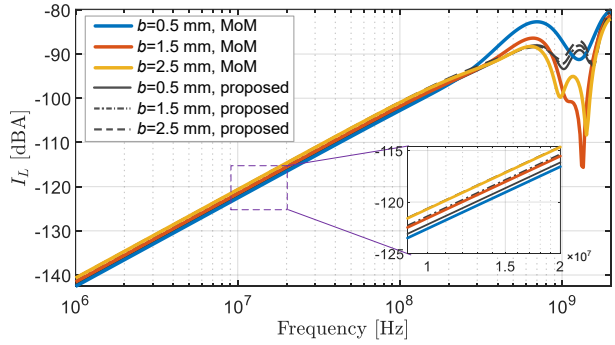

(b)

Figure 5. Prediction of the current induced at the left terminal for different values of b (R=3 cm and L=0.1 m) for (a) δ=180°, and (b) δ=90°.

5 Conclusion

In this work, a TL-based model is introduced to predict field-to-wire coupling in a wiring structure (singled-ended interconnection) with a loop in the middle. To this end, the trajectory of the line conductor is modelled as a curve in the three dimensions, with the local wire orientation used to evaluate the distributed excitation sources induced by the external field. The effectiveness of the proposed approach in predicting the currents induced at the line terminals was investigated for different orientations of the loop. By comparison versus full-wave (MoM) simulations, the presented examples not only prove the effectiveness of the proposed modeling procedure, but also outline the need for accurate modeling of the wire geometry to avoid underestimation of the actual disturbance levels, especially at high frequency.

6 References

1. G. Spadacini, F. Grassi and S. A. Pignari, "Field-to-Wire Coupling Model for the Common Mode in Random Bundles of Twisted-Wire Pairs," in *IEEE Transactions on Electromagnetic Compatibility*, vol. 57, no. 5, pp. 1246-1254, Oct. 2015, doi: 10.1109/TEMC.2015.2414356.

2. X. Liu, F. Grassi, G. Spadacini and S. A. Pignari, "Physically Based Modeling of Hand-Assembled Wire Bundles for Accurate EMC Prediction," in *IEEE Transactions on Electromagnetic Compatibility*, vol. 62, no. 3, pp. 914-922, June 2020, doi: 10.1109/TEMC.2019.2922455.

3. Y. Wang, Y. S. Cao, D. Liu, R. W. Kautz, N. Altunyurt and J. Fan, "Evaluating the Crosstalk Current and the Total Radiated Power of a Bent Cable Harness Using the Generalized MTL Method," in *IEEE Transactions on Electromagnetic Compatibility*, vol. 62, no. 4, pp. 1256-1265, Aug. 2020, doi: 10.1109/TEMC.2019.2927222.

4. J. C. Pincenti, and P. L. Uslenghi, "Incident field excitation of random cables." in *Radio Science*, vol. 42, no. 06, pp. 1-10, 2007, doi: 10.1029/2007RS003662.

5. W. Kühnel, *Differential geometry: Curves – Surfaces – Manifolds*. Vol. 77. American Mathematical Soc., 2015.

6. C. R. Paul, *Analysis of multiconductor transmission lines*. John Wiley & Sons, 2007.

7. A. K. Agrawal, H. J. Price and S. H. Gurbaxani, "Transient Response of Multiconductor Transmission Lines Excited by a Nonuniform Electromagnetic Field," in *IEEE Transactions on Electromagnetic Compatibility*, vol. EMC-22, no. 2, pp. 119-129, May 1980, doi: 10.1109/TEMC.1980.303824.